Computación y Sistemas
ISSN: 1405-5546
computacion-y-sistemas@cic.ipn.mx
Instituto Politécnico Nacional
México

Pérez-Sánchez, Héctor A.; Benítez-Rendón, Edward U.; Castillo-Toledo, Bernardino; Loukianov, Alexander G.; Luque-Vega, Luis F.; Saad, Maarouf
Cockpit Design for First Person View Flight for a Remotely Operated Quadrotor Helicopter
Computación y Sistemas, vol. 19, núm. 3, 2015, pp. 501-511
Instituto Politécnico Nacional
Distrito Federal, México

ISSN 2007-9737

Cockpit Design for First Person View Flight for a Remotely Operated Quadrotor Helicopter

Héctor A. Pérez-Sánchez[1], Edward U. Benítez-Rendón[1], Bernardino Castillo-Toledo[1], Alexander G. Loukianov[1], Luis F. Luque-Vega[2], Maarouf Saad [3]

[1] Instituto Politécnico Nacional, CINVESTAV Campus Guadalajara, Department of Automatic Control, Zapopan, Jalisco, Mexico

[2] ITESO University, Department of Electronics, Systems and Informatics, Tlaquepaque, Jalisco, Mexico

[3] École de Technologie Supérieure, Power Electronics and Industrial Control Research Group, Montreal, Quebec, Canada

{haperez, eubenitez, toledo, louk}@gdl.cinvestav.mx, luisluque@iteso.mx, Maarouf.Saad@etsmtl.ca

Abstract. Recently, technological advances have been focused on the cockpit of modern unmanned aerial vehicles (UAVs) in order to reduce pilot requirements and workload to operate them. First person view (FPV) flight represents a key point when UAVs perform tasks beyond the line of sight. This paper presents the design and implementation of a cockpit for a remotely operated quadrotor. We have developed an intuitive graphical user interface (GUI) for piloting the quadrotor encompassing the most relevant flight instruments as an altimeter, attitude, heading, and ground speed indicators. The GUI is developed using the programming development environment LabVIEW®.

Keywords. Quadrotor, cockpit, block control, LabVIEW®.

1 Introduction

FPV flight is a type of remote control (RC) flying that represents a topic of fast-growing popularity in recent years due to its several applications such as aerial surveillance, infrastructure monitoring, photo, and filming, among others. Performing this type of flight involves the ability of the pilot to see from the aircraft perspective. In order to bring this characteristic to any RC aircraft it is necessary to mount some electronics devices like a small video camera and a video transmitter with the aim of displaying the live video streaming on video goggles or a portable screen. As a result, an FPV aircraft can fly beyond the line of sight from the pilot since he does not have to look at the aircraft.

There are several interesting works focused on the first-person view paradigm in which an intuitive interface is used to provide the pilot with the capability to move the position of a camera to track a specific target image. In [1], an intuitive tangible interface between the pilot and the blimp is developed where a transparent manipulation of an embedded camera is controlled instinctively by the head's movement so that the user is available for other tasks such as piloting the blimp. However, there are tasks where a blimp is not a suitable platform for performing a specific task due to its low maneuverability, therefore, an aerial robotic system constituted by an aircraft is presented in [2] where a low-cost remote vision system provides an FPV to the operators in real time. The aerial system uses a video camera with a wide-angle (fisheye) lens while the pilot is outfitted with virtual goggles with integrated attitude and heading sensors to move a pant-tilt camera unit (PTCU).

Other works explode the capabilities of the combination of a quadrotor and a PTCU as in [3]

and [4]. In [3], a design of a vision-based controller to follow a leader vehicle autonomously is introduced, while [4] presents a nonlinear velocity controller to produce simultaneous complementary motion of the quadrotor and the PTCU. Moreover, a mission-centric approach controlling a quadrotor with four degrees of freedom (DOF) combined with a two-DOF camera kinematic model to create a single system to provide a full six-DOF actuation of the camera view is presented in [5]. The advantage of this approach is the fusion of the vehicle navigation and camera targeting into a single task in which the pilot sees and flies the system as through riding on the camera optical axis.

Two main components have to be considered when an FPV setup is established: the aircraft and the ground station (GS). The complexity of a GS varies from a simple configuration with a monitor connected to a wireless receiver to a more complicated one with things like a diversity receiver, multiple monitors or goggles, video splitters, camcorders, antenna tracking, among others. The process of designing a GUI for a remotely operated quadrotor UAV is investigated in [6] where the orientation of the quadrotor is transmitted to the GS wirelessly. However, current applications need to be performed with a higher level of reliability based on the knowledge of more physical variables before and during flight.

In this work, a GS based on an intuitive cockpit is designed in LabVIEW® programming environment for piloting a remotely operated quadrotor beyond the line of sight. In order to perform a safe FPV flight, the developed GUI encompasses the most relevant flight instruments such as an altimeter, attitude, heading, and ground speed indicators. Moreover, the block control (BC) technique is applied to both manual and autonomous flight.

This paper is organized as follows: in Section 2, the control design for the quadrotor is described. Further on, a description of the FPV aerial system is given in Section 3 showing the quadrotor platform and the design of the cockpit in the ground station. Finally, some conclusions are presented.

2 Control Design for the Quadrotor

2.1 Mathematical Model

The well-known quadrotor configuration has four rotors which generate the propeller forces F_i $(i = 1,2,3,4)$. Each rotor consists of a brushless DC motor and a fixed-pitch propeller. This helicopter is constituted by two rotors rotating counter-clockwise (1, 3) and two rotors rotating clockwise (2, 4). In order to increase the altitude of the aircraft, the rotor speeds have to be increased in the same quantity. Forward motion is accomplished by increasing the speed of the rotors (3, 4) while simultaneously reducing the same value for rotors (1, 2). For rightward motion the speed of rotors (2, 3) is increased while the speed of rotors (1, 4) is reduced. Backward and rightward motion can be accomplished similarly. Finally, yaw motion can be performed by speeding up or slowing down the clockwise rotors depending on the desired angle direction. The main objective of the quadrotor prototype is to perform the FPV flight mode, therefore, the coordinate axes describing the kinematic model of the quadrotor with the ×-configuration are shown in Fig. 1.

The dynamic nonlinear model describing the quadrotor behavior in its state space representation form [7] is given by

$$\dot{X} = f(X, U), \tag{1}$$

with the state vector

$$\begin{array}{llll} x_1 = \varphi & x_2 = \dot{\varphi} & x_3 = \theta & x_4 = \dot{\theta}, \\ x_5 = \psi & x_6 = \dot{\psi} & x_7 = z & x_8 = \dot{z}, \\ x_9 = x & x_{10} = \dot{x} & x_{11} = y & x_{12} = \dot{y}, \end{array}$$

where $x, y,$ and z represent the relative position of the center of gravity of the quadrotor, and $\varphi, \theta,$ and ψ represent the three Euler angles (roll, pitch, and

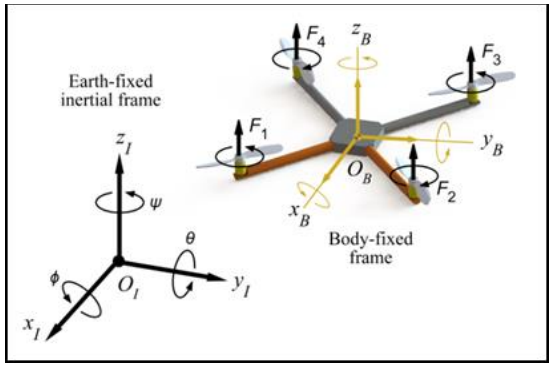

Fig. 1. Quadrotor with ×-configuration

yaw) that define the orientation of the quadrotor with respect to the inertial frame $\{I\}$. The control inputs are defined as

$$U_1 = \frac{1}{\sqrt{2}}(-F_1 + F_2 + F_3 - F_4),$$
$$U_2 = \frac{1}{\sqrt{2}}(-F_1 - F_2 + F_3 + F_4),$$
$$U_3 = -F_1 + F_2 - F_3 + F_4,$$
$$U_4 = F_1 + F_2 + F_3 + F_4.$$

and the function $f(X,U)$ is given as

$$(X,U) = \begin{bmatrix} x_2 \\ p_1 + b_1 U_1 \\ x_4 \\ p_2 + b_2 U_2 \\ x_6 \\ p_3 + b_3 U_3 \\ x_8 \\ -g + \frac{\mathrm{C}\,x_1\,\mathrm{C}\,x_3}{m} U_4 \\ x_{10} \\ \frac{U_4}{m} u_x \\ x_{12} \\ \frac{U_4}{m} u_y \end{bmatrix},$$

where

$$p_1 = x_4 x_6 a_1 + x_4 a_2 \omega,$$
$$p_2 = x_2 x_6 a_3 + x_2 a_4 \omega,$$
$$p_3 = x_2 x_4 a_5,$$

$$u_x = \mathrm{C}\,x_1\,\mathrm{S}\,x_3\,\mathrm{C}\,x_5 + \mathrm{S}\,x_1\,\mathrm{S}\,x_5, \quad (2)$$
$$u_y = \mathrm{C}\,x_1\,\mathrm{S}\,x_3\,\mathrm{S}\,x_5 - \mathrm{S}\,x_1\,\mathrm{C}\,x_5,$$

$$b_1 = \frac{d}{I_x}, \quad b_2 = \frac{d}{I_y}, \quad b_3 = \frac{1}{I_z},$$

$$a_1 = \frac{I_y - I_z}{I_x}, \quad a_2 = -\frac{J_R}{I_x}, \quad a_3 = \frac{I_z - I_x}{I_y},$$

$$a_4 = \frac{J_R}{I_y}, \quad a_5 = \frac{I_x - I_y}{I_z}.$$

We consider the following two control problems for the quadrotor platform: manual and autonomous flight. The first one involves the control of the altitude and attitude variables (Euler angles) of the quadrotor, while the second one involves the absolute position (latitude, longitude, and altitude) and the yaw angle. These flight controllers are explained in detail in the following subsections. It is important to notice that both flight controllers can be used when performing FPV flight, the main difference between using any of them lies in the level of dependency on the pilot.

2.2 Control Design

The control algorithm design in this subsection is carried out using the block control (BC) technique [8].

2.2.1 Manual Flight

In order to achieve manual flight, the controller has to ensure the asymptotic convergence of the output vector $y_1 = [x_1, x_3, x_5, x_7]^T$ to the reference trajectory vector $y_{1r} = [x_{1r}, x_{3r}, x_{5r}, x_{7r}]^T$. Then, we can define the tracking error as

$$z_1 = y_{1r} - y_1. \quad (3)$$

Further on, taking the time derivative of (3) and using (1) we obtain

$$\dot{z}_1 = \dot{y}_{1r} - y_2, \quad (4)$$

where $y_2 = [x_2, x_4, x_6, x_8]^T$.Then, following the BC technique, the virtual control input y_2 is designed as follows to stabilize the dynamics of z_1:

$$y_2^* = \dot{y}_{1r} + K_1 z_1, \quad (5)$$

with $K_1 = \mathrm{diag}(k_1, k_3, k_5, k_7)$, and $k_i > 0$, $i = 1,3,5,7$. Defining $z_2 = y_2^* - y_2$ and using (5) and (1), we get

$$\dot{z}_2 = \ddot{y}_{1r} + K_1 \dot{z}_1 - \bar{f}_1 - B_1 U, \quad (6)$$

where $\bar{f}_1 = [p_1, p_3, p_5, -g]^T$, the control coefficient matrix is $B_1 = \mathrm{diag}(b_1, b_2, b_3, \mathrm{C}\,x_1\,\mathrm{C}\,x_3/m)$, and the control input vector is $U = [U_1, U_2, U_3, U_4]^T$. Now, we choose the control input U in (6) introducing the desired dynamics:

$$U = B_1^{-1}\left(\ddot{y}_{1r} + K_1 \dot{z}_1 - \bar{f}_1 + K_2 z_2\right), \quad (7)$$

with $K_2 = \mathrm{diag}(k_2, k_4, k_6, k_8)$, and $k_{i+1} > 0$, $i = 1,3,5,7$. It can be noted that the inverse of B_1 exists if the following constraints hold: $-\pi/2 \leq x_j \leq \pi/2$, $j = 1,3,5$. It can also be noted that the remain dynamics containing the x and y position of the quadrotor are not taken into account for manual flight.

2.2.2 Autonomous Flight

For achieving autonomous flight, it is necessary to generate the desired pitch and roll angles to drive the helicopter to the desired longitudinal and latitudinal position, respectively. Let us define the output vector $y_3 = [x_9, x_{11}]^T$ and the reference trajectory vector $y_{3r} = [x_{9r}, x_{11r}]^T$, then we can define the tracking error as

$$z_3 = y_{3r} - y_3. \tag{8}$$

Further on, taking the time derivative of (8) and using (1) we obtain

$$\dot{z}_3 = \dot{y}_{3r} - y_4, \tag{9}$$

where $y_4 = [x_{10}, x_{12}]^T$. Then, the virtual control input y_4 is designed as follows to stabilize the dynamics of z_3:

$$y_4^* = \dot{y}_{3r} + K_3 z_3, \tag{10}$$

with $K_3 = \text{diag}(k_9, k_{11})$ and $k_t > 0,\ t = 9{,}11$. Defining $z_4 = y_4^* - y_4$ and using (10) and (1), we get

$$\dot{z}_4 = \ddot{y}_{3r} + K_3 \dot{z}_3 - B_2 U^*, \tag{11}$$

where $B_2 = \text{diag}(U_4/m, U_4/m)$ and the control input vector is $U^* = \left[u_x^*, u_y^*\right]^T$. Now, we choose the control input U^* in (11) introducing the desired dynamics:

$$U^* = B_2^{-1}(\ddot{y}_{3r} + K_3 \dot{z}_3 + K_4 z_4), \tag{12}$$

with $K_4 = \text{diag}(k_{10}, k_{12})$, and $k_{i+1} > 0, i = 9{,}11$.

Then, it is easy to find the desired pitch angle (x_{3_d}) and the roll angles (x_{1_d}) from (12) and (2). These angles are given as

$$\begin{aligned} x_{1_d} &= \sin^{-1}\left(u_x^* \sin x_5 - u_y^* \cos x_5\right), \\ x_{3_d} &= \sin^{-1}\left(\frac{u_x^* - \sin x_1 \sin x_5}{\cos x_1 \cos x_5}\right). \end{aligned} \tag{13}$$

Finally, $y_{1r} = [x_{1r}, x_{3r}, x_{5r}, x_{7r}]^T$ defining the reference trajectory vector is changed to the vector $y_{1r}^* = [x_{1d}, x_{3d}, x_{5r}, x_{7r}]^T$. Then, the autonomous flight controller will use the algorithm developed for manual flight as an inner control.

3 Description of the FPV Aerial System

One of the main goals while performing the FPV flight mode with the quadrotor is to increase the range of the complete unmanned aerial system. Therefore, the complete system architecture is devoted to perform this task with the knowledge of the helicopter variables at every moment. There are two primary components of our FPV setup: the quadrotor and the GS. The quadrotor has a diagonal wheelbase of 450 mm, weighing 1790 g, and flying time of 14 min. The ground station runs on a Windows 7 with core i3 at 2.3 GHz and 8 GB RAM. These two components are shown in Fig. 2.

The hardware architecture is depicted in Fig. 3. It can be noted that the flight controller on the quadrotor requires an on-board processor,

Fig. 2. FPV flight system at CINVESTAV Guadalajara

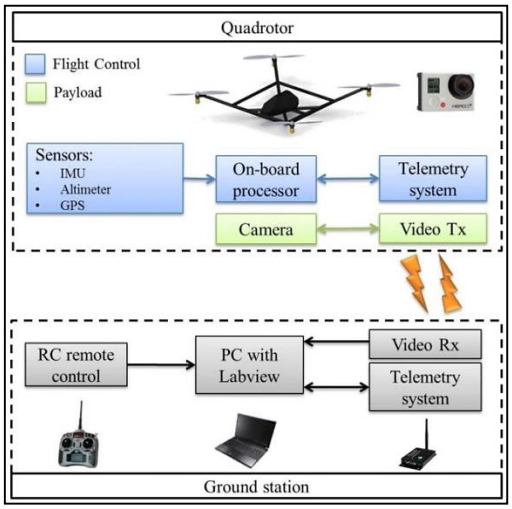

Fig. 3. Hardware architecture for FPV flight

sensors, and the telemetry system based on radio frequency. This flight controller is responsible for the task management, sensor fusion, and translating the flight control instructions into a robust and safe flight. Besides, the GS provides the user the ability to monitor the variables of the helicopter during the flight through an intuitive GUI; this represents the main contribution of our work.

The above mentioned parts will be described in detail in the following subsections.

3.1 Quadrotor Helicopter

The quadrotor helicopter is classified as a powered rotary wing vertical take-off and landing (VTOL) aircraft. The quadrotor is equipped with an autopilot which consists of a microprocessor, an inertial measurement unit (IMU), GPS, altimeter, and a telemetry system. An IMU encompasses a 3-axis gyroscope, a 3-axis accelerometer, and a 3-axis magnetometer. The quadrotor flight controller is able to perform the two flying modes mentioned in Section 2: manual flight and autonomous flight. Moreover, several robust flight controllers have been carried out in our lab for the quadrotor aerial platform [9, 10].

3.2 Ground Station

Monitoring the quadrotor during flight represents the key point in the development of this work. The ground station is equipped with an RC remote control, a laptop, the telemetry system, and the video receiver. The mentioned hardware is kept to the minimum required hardware for performing FPV flight. The GS software involves the design of a cockpit which serves as the GUI between the pilot and the quadrotor; it is primarily responsible for monitoring and sending data to the helicopter. The GS displays the instrumentation (physical parameters) of the helicopter via a GUI developed using the programming development environment LabVIEW®. The GS is shown in Fig. 4.

Reliable flight instrumentation is crucial to conducting safe flight operations and it is important that the pilot has a basic understanding of their operation. The basic flight instruments required for operation under visual flight rules (VFR) are

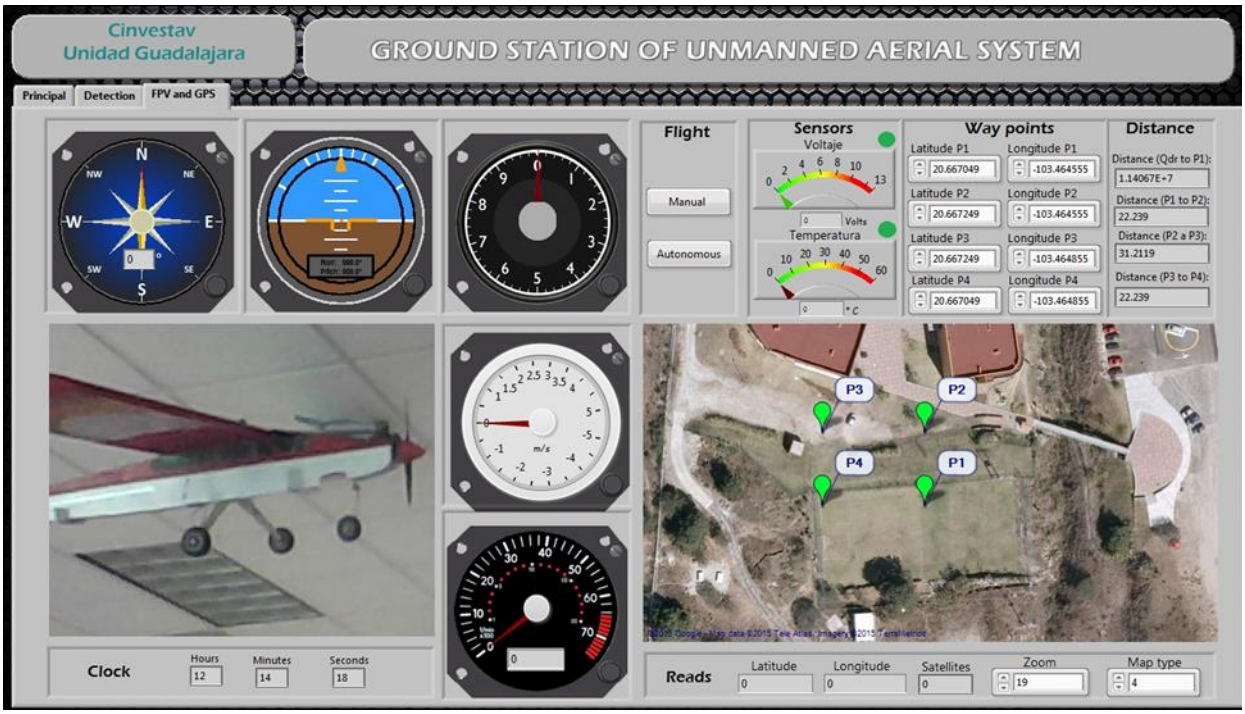

Fig. 4. Graphical user interface of the ground station

altimeter, and attitude and heading indicator [11]. The flight instruments considered for the proposed cockpit are described in the subsections that follow.

3.2.1 Static Systems

Altimeter: a sensitive altimeter shown in Fig. 5 is a barometer sensor that measures the absolute pressure of the ambient and displays it in terms of meters above a selected pressure level [11].

Vertical Speed Indicator (VSI): the VSI is also called a vertical velocity indicator (VVI), it was formerly known as a rate-of-climb indicator (see Fig. 6). This instrument gives an indication of any deviation from a constant pressure level. The measurement is obtained by means of filtering the position obtained with the barometer sensor. This indicator is useful in alerting the pilot of an upward or downward trend.

Ground speed: it is the horizontal speed in which the aircraft moves relative to a fixed point on the ground. This variable can be directly measured using the GPS system by measuring the elapsed time between passing two points on the ground. Fig. 7 depicts the ground speed meter.

3.2.2 Gyroscopic Instruments

Gyroscopic systems allow to describe the orientation of the helicopter in three axes (x, y, z) denominated (roll, pitch, yaw), respectively.

Attitude Indicator: the first attitude instrument (AI) was originally referred to as an artificial horizon; it is also known as gyro horizon or attitude director indicator as shown in Fig. 8. This instrument is used to inform the pilot about the orientation of the aircraft relative to the Earth's horizon. It indicates pitch (fore and aft tilt) and bank or roll (side to side tilt).

Heading Indicator: the heading of the rotorcraft indicates the direction of the quadrotor´s nose. The accelerometer, gyroscope, and magnetometer work in unison to provide a fairly accurate picture of where the quadrotor´s nose is pointed to. The magnetometer gives us a fixed reference point (magnetic north), and then this measurement is used to re-calibrate the drift in the gyroscope due to the elapsed time yielding to a more accurate measurement. This indicator is depicted in Fig. 9.

Fig. 5. Altimeter indicator

Fig. 6. Vertical speed indicator

Fig. 7. Cruise speed indicator

Fig. 8. Attitude indicator

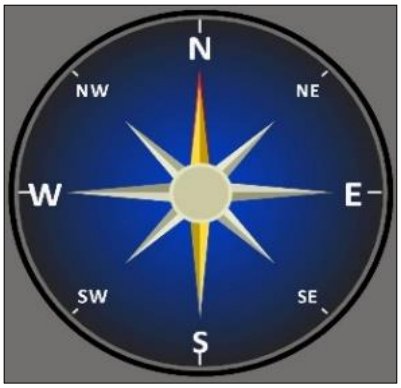

Fig. 9. Heading indicator

Fig. 10. Cross-checking

The order of the indicators for the design in the GS is defined following the method known as cross-checking: it is a continuous and logical observation of instruments for attitude and performance information. In attitude instrument flying, an attitude is maintained by reference to the instruments, which produces the desired result in performance. These variables make it necessary to constantly check the instruments and make appropriate changes in the helicopter's attitude [11]. This GS concentrates on the six basic flight instruments shown in Fig. 10.

3.2.3 Additional Instruments

There is additional instrumentation that has to be taken into account to ensure a more reliable flight when performing FPV flight.

Location indicator: the GPS is a satellite- based radio navigation system which provides unequalled accuracy and flexibility in positioning for navigation, surveying, and GIS (Geographic Information system) data collections [12]. The GPS navigation system broadcasts a signal that is used by receivers to determine precise position anywhere in the world. The receiver tracks multiple satellites and determines a pseudo range measurement to determine the user location. A minimum of four satellites is necessary to establish an accurate three-dimensional position [11]. A location map is a useful tool for introducing an FPV system (see Fig. 11); this will enable the monitoring of the current aircraft position. The location map is based on an application programing interface (API) linked to Google Maps. The GPS receiver is placed on the vehicle. The GPS tab provides a location map on which there are two markers that indicate the origin of the takeoff and the current vehicle position, each one with its corresponding label. Also, visible indicators are used to choose the type of map, a map zoom selector, and indicators linked satellite number, latitude and longitude of the vehicle.

The accuracy of the GPS depends on whether we are talking about standalone (single receiver) or differential positioning, single or dual frequency receivers, real-time or post-processed operation, and so on [13]. Moreover, the horizontal dilution of precision (HDOP) is a measurement of accuracy in a two-dimensional horizontal position. The HDOP

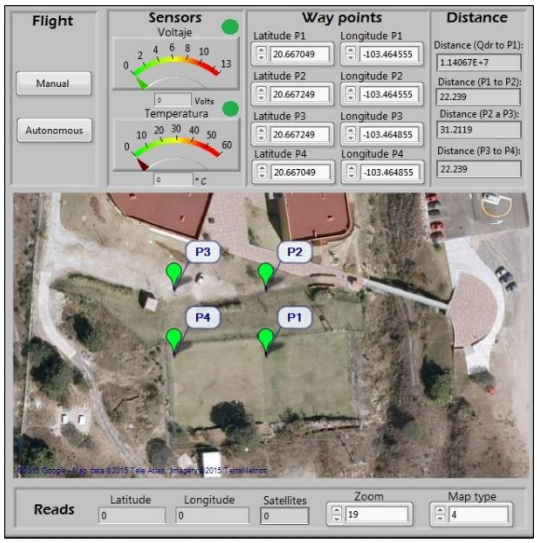

Fig. 11. Navigation system

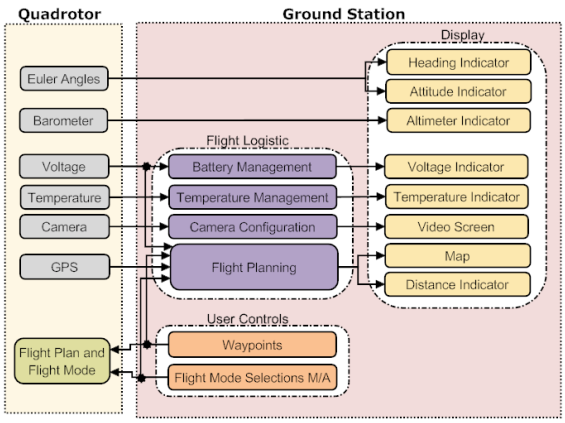

Fig. 12. Block diagram of the GS

is important in evaluating GPS surveys intended for horizontal control. The HDOP is basically the error determined from the final variance covariance matrix divided by the standard error of the range measurements. HDOP roughly indicates the satellite range geometry on a resultant position [12].

Battery indicator: the introduction of a voltage sensor helps people reduce failures that could occur to the vehicle by low battery voltage. Some of the failures that might come to reach a low battery voltage are presence of Brown-outs on the control board, the ESC fail, and the engines stopped due to a lack of signal from the ESC. The implementation of the battery indicator is intended to protect the vehicle against the flaws mentioned above; this indicator will alert the driver that the vehicle has a low voltage. The alert has been considered to occur in two situations: in flight and before takeoff.

- If the alert is presented in flight, the pilot shall have a voltage tolerance (a voltage set by the pilot) to achieve a safety landing.
- If the alert is present before takeoff, the vehicle engine will block until the user changes the discharged battery with a charged one.

Temperature indicator: the control card which is placed in the center of the vehicle is affected by such factors as temperature and humidity. It was considered that the pilot must have knowledge of the temperature where you are operating the control board due to the following circumstances:

- The temperature affects the performance of the electronic devices on the onboard card.
- High temperatures may indicate that the control board or some of its components could be damaged.

Therefore, to eliminate the possibility of faults due to exceeding the nominal temperature conditions, it is pertinent to add this temperature gauge.

In summary, the GS serves not only as a graphical user interface to monitor the physical variables of the quadrotor during flight, but it can also be used to plan the feasibility of the flight. The block diagram explaining the interconnections in the GS is depicted in Fig. 12.

4 Flight test

Several experiments were carried out for evaluating the performance of the complete FPV system. In particular, one flight test encompassing both manual and autonomous flight is demonstrated. The quadrotor takes off in the manual mode and once we achieve 20m we switch to the autonomous flight mode in order to yield a distance of 70 m away from the home position; it should be noted that the user has the capability to

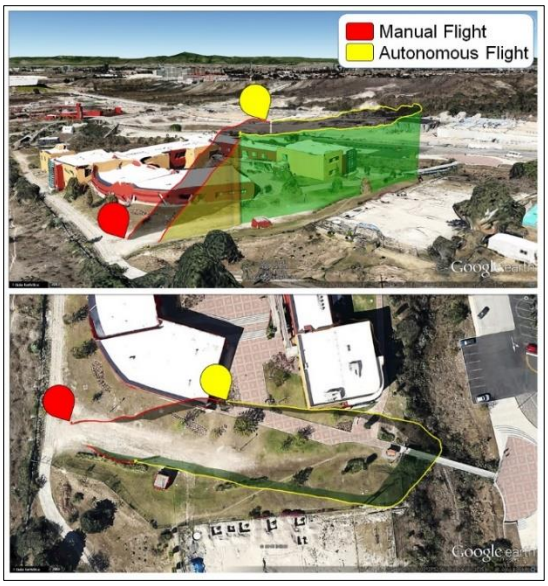

Fig. 13. GPS location of the quadrotor during FPV flight

change the flight direction of the quadrotor at any moment during the entire flight.

Once the flight is completed it is possible to display the trajectory of the quadrotor using Google Earth, this is shown in Fig. 13.

The processing time in LabVIEW® is critical since the quadrotor has a fast dynamics. In order to withstand this, the quadrotor is programmed to reduce the sensibility on the sticks when it is in the manual mode and to reduce its cruise speed when it is in the autonomous flight mode.

5 Conclusions

The implementation of the GS based on a cockpit to remotely operate the quadrotor helicopter in the programming environment LabVIEW® has clear advantages over the classical FPV goggles systems. These advantages are fast implementation, lower-cost, and robustness. The developed GUI is used for monitoring the quadrotor position and orientation with a high level of reliability. Moreover, its use is very intuitive for the pilot, which reduces the training period and the workload to operate the whole aerial system. Currently, the effects of communication delays between the quadrotor and the GS are being investigated in our group.

Acknowledgements

This work was supported by the National Council on Science and Technology (CONACYT), Mexico, under grants 127858 and 129591.

References

1. **Righetti, X., Cardin, S., Thalmann, D., & Vexo, F. (2007).** Immersive flight for surveillance applications. *IEEE Symposium on 3D User Interfaces,* (3DUI'07), doi: 10.1109/3DUI.2007.340786.
2. **Marine, P.M. & Rawashdeh, O.A. (2010).** A First-Person View System for Remotely Operated Vehicles Using a Fisheye-Lens. *AIAA Infotech at Aerospace,* Atlanta, Georgia, doi: 10.2514/6.2010-3513.
3. **Chitrakaran, V., Dawson, D., Kannan, H., & Feemster, M. (2006).** Vision Assisted Autonomous Path Following for Unmanned Aerial Vehicles. *45th IEEE Conference on Decision and Control,* pp. 63–68.
4. **Neff, A., Lee, D., Chitrakaran, V., Dawson, D., & Burg, T. (2007).** Velocity control for a quad-rotor uav fly-by-camera interface. *IEEE Southeast Conf.,* pp. 273–278, doi: 10.1109/SECON.2007.342901.
5. **Lee, D., Chitrakaran, V., Burg, T., Dawson, D., & Xian, B. (2007).** Control of a remotely operated quadrotor aerial vehicle and camera unit using a fly-the-camera perspective. *46th IEEE Conference on Decision and Control, pp.* 6412–6417, doi: 10.1109/CDC.2007.4434940.
6. **Zul Azfar, A. & Hazry, D. (2011).** Simple GUI design for monitoring of a remotely operated quadrotor unmanned aerial vehicle (UAV). *7th International IEEE Colloquium on Signal Proc. and its Applications* (CSPA), pp. 23–27, doi: 10.1109/CSPA.2011.5759836.
7. **Bouabdallah, S. & Siegwart, R. (2005).** Backstepping and Sliding-mode Techniques Applied to an Indoor Micro Quadrotor. *IEEE International Conference on Robotics and Automation (ICRA 2005),* pp. 2247–2252, doi: 10.1109/ROBOT.2005.1570447.
8. **Loukianov, A.G. (2002).** Robust block decomposition sliding mode control design. *Mathematical Problems in Engineering,* Vol. 8, pp. 349–365, doi: 10.1080/10241230306732.

9. **Luque-Vega, L., Castillo-Toledo, B., & Loukianov, A.G. (2012).** Robust block second order sliding mode control for a quadrotor. *Journal of the Franklin Institute (Advances in Guidance and Control of Aerospace Vehicles using Sliding Mode Control and Observation Techniques),* Vol. 349, No. 2, pp. 719–739.
10. **Luque-Vega, L.F. (2010).** *Design, Construction and Control of a Quadrotor Helicopter.* Master thesis, CINVESTAV del IPN Unidad Guadalajara, Guadalajara, Jalisco, Mexico.
11. **Federal Aviation Administration (2008).** *Pilot´s Handbook of Aeronautical Knowledge.* Government Printing Office, United States.
12. **Gopi S. (2005).** Global *Positioning System: Principles And Applications.* McGraw-Hill Education, India.
13. **Langley, R.B. (1999).** Dilution of precision. *GPS world,* Vol. 10, pp. 52–59.

Héctor A. Pérez-Sánchez received his B.Sc. degree in Electronic Engineering from the Technological Institute of Tuxtla Gutierrez, Chiapas, Mexico. He currently works at the Advanced Studies and Research Center of the National Polytechnic Institute, Campus Guadalajara, Mexico, as research assistant in the Unmanned Aerial System project with the Autonomous Vehicles Laboratory. His main research interests focus on software development for flight controllers in unmanned aerial vehicles.

Edward U. Benítez Rendón received his B.Sc. degree in Electronic Engineering from the Technological Institute of Tuxtla Gutierrez, Chiapas, Mexico. He currently works at the Advanced Studies and Research Center of the National Polytechnic Institute, Campus Guadalajara, Mexico, as research assistant in the Unmanned Aerial System project with the Autonomous Vehicles Laboratory. His research interests include multicopter design and navigation control.

Bernardino Castillo-Toledo received his B.Sc. degree in Electrical Engineering from the National Polytechnic Institute (IPN), Mexico City, Mexico, the M.Sc. degree from the Research and Advanced Studies Center of the National Polytechnic Institute (CINVESTAV-IPN), Guadalajara, Mexico, and the Ph.D. degree from the University of Rome "La Sapienza," Rome, Italy, in 1981, 1985, and 1992, respectively. He was a Lecturer with the School of Electrical and Mechanics Engineering, IPN, from 1985 to 1989. From 1985 to 1995, he was with the Automatic Control Section, Department of Electrical Engineering, CINVESTAV-IPN, and, since 1995, with CINVESTAV-IPN, Guadalajara Campus. He had several research stays with the University of Rome "La Sapienza" and the University of L'Aquila, L'Aquila, Italy, and was a visiting Professor at the Laboratoire d'Automatique et d'Analyse des Systemes, French Council for Scientific Research, from 1999 to 2000, and at the University of Compiègne, Compiegne, France, during the first semester of 2002. His main research interests include nonlinear control design, the robust regulation problem, and the application of artificial neural networks and fuzzy logic techniques to control and fault diagnosis of dynamical systems.

Alexander G. Loukianov received his B.Sc. degree from the Polytechnic Institute, Moscow, Russia, in 1975, and the Ph.D. degree in Automatic Control from the Institute of Control Sciences, Russian Academy of Sciences, Moscow, Russia, in 1985. He was with the Institute of Control Sciences in 1978 and was the Head of the Discontinuous Control Systems Laboratory from 1994 to 1995. From 1995 to 1997, he held a visiting position at the University of East London, London, U.K., and since April 1997, he has been with the Research and Advanced Studies Center of the National Polytechnic Institute, Guadalajara Campus, Mexico, as a Professor of Electrical Engineering graduate programs. From 1992 to 1995, he was in charge of a joint industrial project of the institute and the largest Russian car plant and also of several international projects supported by the International Association and Specific International Scientific Cooperation Activities-COPERNICUS, Brussels. He has published more than 100 papers in international journals, books, and conferences and has been a reviewer for different international journals and conferences. His research interests include nonlinear system robust control and variable structure systems with sliding modes as applied to dynamical plants with delay, electric drives, power systems control, robotics, spice, and automotive control.

Luis F. Luque Vega received his B.Sc. degree in Electronic Engineering from the Technological Institute of Culiacan, Sinaloa, Mexico, the M.Sc. degree, and the Ph.D. degree in Electrical Engineering from the Advanced Studies and Research Center of the National Polytechnic Institute, Campus Guadalajara, Mexico, in 2007, 2010, and 2014, respectively. He is currently a postdoctoral fellow in ITESO University at the Department of Electronics, Systems, and Informatics. His research interests include non-linear robust control design, sliding modes and their applications to robotics and flight control systems.

Maarouf Saad received the B.Sc. and M.Sc. degrees in Electrical Engineering from École Polytechnique of Montréal, Montreal, QC, Canada, in 1982 and 1984, respectively, and the Ph.D. degree in Electrical Engineering from McGill University, Montreal, in 1988. In 1987, he joined École de Technologie Supérieure, Montreal, where he currently teaches control theory and robotics courses. His research is mainly in nonlinear control and optimization applied to robotics and flight control system.

Article received on 07/12/2014; accepted on 15/04/2015.
Corresponding author is Héctor A. Pérez-Sánchez.